

## Surface Radiation Budget from Satellites

R. T. PINKER AND L. A. CORIO

*Department of Meteorology, University of Maryland, College Park, MD 20742*

(Manuscript received 13 October 1982, in final form 19 August 1983)

### ABSTRACT

The net radiation received at the ground serves as a pseudoforcing function for the exchange of energy at the ground-air interface. Yet, information regarding this parameter is not available on a routine basis. In this study an attempt is being made to demonstrate that satellite inferred information might be useful for the estimation of radiation budget parameters at the ground surface. Observations from the NOAA 5 satellite were utilized to relate planetary radiation budget parameters to surface net radiation, over the central United States. The net radiation and the outgoing IR radiation at the top of the atmosphere were found to be correlated to the net radiation at the surface, yielding a multiple correlation coefficient of 0.76.

### 1. Introduction

The net gain or loss of radiant energy at the ground surface is an important entity. Information regarding this parameter is relevant to problems dealing with regional climate trends (Budyko, 1974), as well as solar energy applications and agriculture. However, the net radiation is not routinely measured. Previous attempts to derive it on a regional scale were based on approximate parameterization schemes which utilized global solar radiation data and observed meteorological inputs (i.e., Linacre, 1968; Lettau, 1969; Hare, 1980). Even this simplified approach is not readily applicable on the mesoscale, since the required inputs are available at most on the macroscale. The variability in the distribution of global solar radiation is, however, on a much smaller scale. In a World Meteorological Organization (WMO) report Gandin (1970) suggested that the desired distance between global solar radiation monitoring stations should be 150–200 km. Thus, attempts to fill the needs for more detailed information on radiation budget parameters at the surface by using satellite data seems timely. They also conform to the recommendations of various scientific communities, e.g., the Workshop on Earth Radiation Budget Science, 1978, held in Williamsburg, Virginia, to conduct special studies leading to the capability to measure surface radiation budgets from satellites by 1985 (NASA, 1979). Among the specific tasks proposed was the assessment of the ability to determine from satellites the net surface radiation.

In this study an attempt is made to derive simultaneous mesoscale net radiation fields at the surface and at the top of the atmosphere (where it is observed from satellites) and then to develop a methodology for deriving the net radiation field at the surface from satellite observations.

### 2. Present study

#### a. Data

It is difficult to obtain simultaneous mesoscale net radiation fields at the top of the atmosphere and at the ground surface. The net surface radiation  $R_n$  is not available; however, it can be expressed as

$$R_n = (1 - \alpha)(S + s^*) + R_A - R_G, \quad (1)$$

where  $S$ ,  $s^*$  is the shortwave direct and diffuse radiation;  $R_A$ , the longwave atmospheric thermal radiation;  $R_G$ , the longwave terrestrial thermal radiation and  $\alpha$ , is surface albedo. Consequently, a compromise approach can be adopted in which only the net shortwave radiation is obtained from observations, while the net longwave radiation is modeled.

The most suitable data for the application of this approach seemed to be that prepared by Tarpley *et al.* (1978) in their Great Plains experiment. In that experiment the National Oceanic and Atmospheric Administration (NOAA)/National Earth Satellite Service (NESS) collected digital images from the visible channel (0.55–0.75  $\mu\text{m}$ ) of the Geostationary Operational Environmental Satellite (GOES-E)/Visible Infrared Sounding Scanning Radiometer (VISSR), averaged over 50 km  $\times$  50 km target areas over the Great Plains during the summer of 1977. The Great Plains Agricultural Council provided a coincident set of pyranometer data at 33 ground stations (Fig. 1). The ground information was supplemented by global solar radiation data from the NOAA network, as reported in *Monthly Summary Solar Radiation Data*, NOAA/Environmental Data and Information Service (EDIS), National Climate Center (NCC), Asheville, N.C. Cloud cover and temperature data necessary for computing the effective longwave radiation came from the *Monthly*

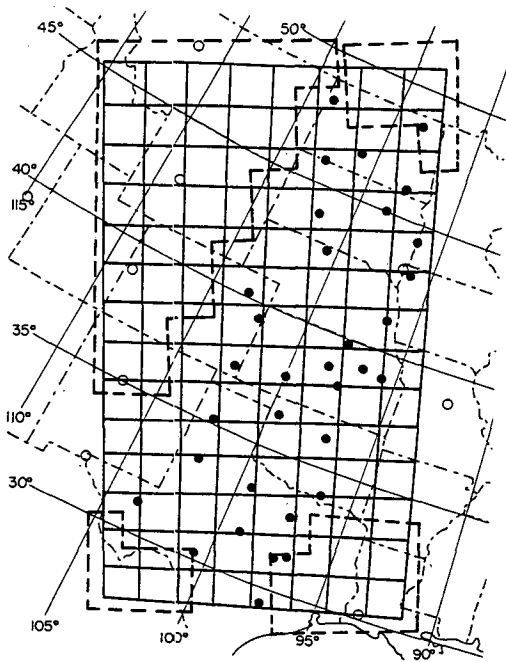


FIG. 1. The NMC (National Meteorological Center) grid and the global solar radiation observation stations of the GPAC (Great Plains Agricultural Council) during the 1977 summer experiment (solid circles), supplemented by NOAA stations (open circles). Grid points within the boxed areas were not used in the statistical analysis due to insufficient density of surface observations.

*Climatological Data Summaries and the Local Climatological Data Summaries*, available for the following 21 stations of interest: 1) Wink, 2) Eldorado, 3) Dallas, 4) Lubbock, 5) Waco, 6) Amarillo, and 7) El Paso, Texas; 8) Manhattan and 9) Dodge City; Kansas; 10) Lander, Wyoming; 11) Grand Junction and 12) Akron, Colorado; 13) Valentine, Nebraska; 14) Sioux Falls, South Dakota; 15) Bismark, North Dakota; 16) Ely, Nevada; 17) Lake Charles, Louisiana; 18) Columbia, Missouri; 19) Gage, Oklahoma; 20) Albuquerque, New Mexico; and 21) Great Falls, Montana.

An overlapping data base from the NOAA 5 operational polar orbiting satellite (Gruber, 1978; Winston *et al.*, 1979), as archived on the National Meteorological Center (NMC) polar stereographic projection grid with a 102 km resolution at the equator and a 204 km resolution near the poles (Fig. 1), served for computing the energy budgets at the top of the atmosphere.

The archived radiation budget parameters were obtained from observations taken by the two-channel scanning radiometer aboard the NOAA 5 satellite, which has a 2100 local time northbound equator crossing and a 0900 local time southbound equator crossing. The IR channel had an onboard calibration system, while the visible channel was calibrated using laboratory data. In the IR the calibrated signal is expressed as equivalent blackbody temperature. The

procedure for the determination of the total outgoing flux from the radiance measurements in the window region utilizes regression models developed by Abel and Gruber (1979). Assuming isotropy, reflectance can be obtained from the visible channel observations; the reflectance is then accepted as a measure of the daily average albedo. Since satellite-derived radiation budget parameters can have systematic errors due to calibration, degradation of the sensors, spurious errors, and errors resulting from the simplifying assumptions in the different algorithms, it is extremely difficult to quantitatively estimate these errors.

#### b. The net radiation field at the surface

As evident from Eq. (1), the net radiation can be evaluated from the total global shortwave radiation, surface albedo and net longwave radiation. The shortwave radiation was available from the experiment described by Tarpley (1979). The surface albedo (for the summer season) as observed by Kung *et al.* (1964) over that region was used. The following two methods for deriving the net longwave radiation were tested for selected locations in the Great Plains for three summer months (June, July and August) of 1977: a) the Monteith-Idso (MI) model (Monteith, 1960; Idso and Jackson, 1969); b) the Brunt (1932) model. The empirically derived constants in the Brunt model were replaced by those of Sellers (1965) as implemented by Willmott *et al.* (1978).

The differences obtained using the two methods were not significant; subsequently, the MI approach was adopted and is briefly outlined in the remainder of this subsection.

The net longwave radiation was presented by Monteith (1960) as

$$R_A - R_G \equiv LW_N = (1 - C)(\epsilon - 1)\sigma T_A^4 - \Delta L, \quad (2)$$

where  $C$  is the fractional cloud amount;  $\epsilon$ , effective emissivity of the atmosphere;  $\sigma$ , Stefan-Boltzmann constant;  $T_A$ , air temperature at shelter level in Kelvins;  $\Delta L$ , correction constant due to differences between air temperature at shelter level and surface temperature (for June, July and August the values are 9.68, 7.75, and 3.40  $W m^{-2}$  respectively).

Cloudiness is taken into account, through the term  $(1 - C)$ , where  $C$  is the fractional cloud amount. This does not account for the upward longwave radiation that is absorbed by the clouds and re-emitted at cloud base temperature. In Monteith's equation, atmospheric thermal radiation depends upon shelter temperature. Since cloud base temperature is below shelter temperature during the summer months, the thermal atmospheric radiation will be overestimated. Based upon statistics presented by Monteith (1961), the net longwave radiation will be overestimated by about 10%.

The monthly correction constants in Monteith's (1961) study were determined from correlation with

measured net radiation. Such data are not available for the Great Plains. It seemed that using the correction constants derived in England would be preferred to using no corrections.

The emissivity of the ground was assumed to be one. As evident from Eq. (2), the atmospheric thermal radiation depends upon the effective emissivity of the atmosphere, which in turn depends upon the amount of precipitable water in the atmosphere. Since precipitable water is often not available, Idso and Jackson's (1969) parameterization of atmospheric emissivity as a second order polynomial in surface temperature was adopted, namely:

$$\epsilon = 1 - c \exp[-d(273 - T_A)^2]. \quad (3)$$

The coefficients  $c$  and  $d$  were determined by Idso and Jackson from a statistical analysis of experimental data from Phoenix, Arizona; Point-Barrow, Alaska; Aspendale and Kerang, Australia; and, the Indian Ocean, and set equal to 0.261 and  $7.77 \times 10^{-4}$ , respectively. Substituting  $\epsilon$  from Eq. (3) into Eq. (2) yields, in langley's per day,

$$LW_N = (C - 1)c \exp[-d(273 - T_A)^2] \sigma T_A^4 - \Delta L. \quad (4)$$

The resulting average net radiation field over the Great Plains for the three summer months of 1977 is presented in Fig. 2. The corresponding global solar radiation field is illustrated in Fig. 3.

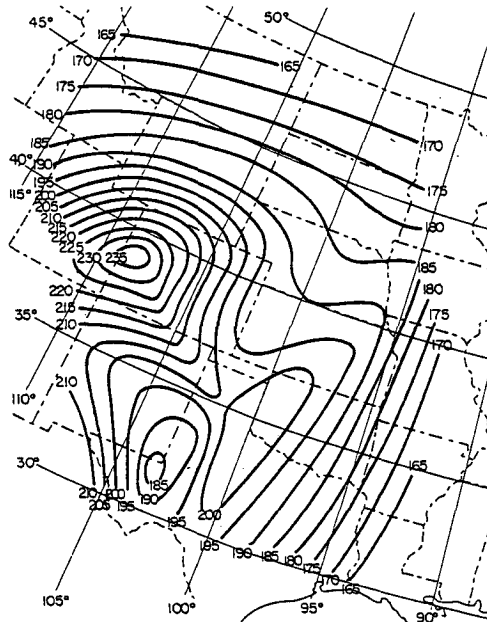


FIG. 2. The surface net radiation ( $W m^{-2}$ ) averaged for three summer months (June–August, 1977) as obtained from measured shortwave radiation and modeled net longwave radiation.

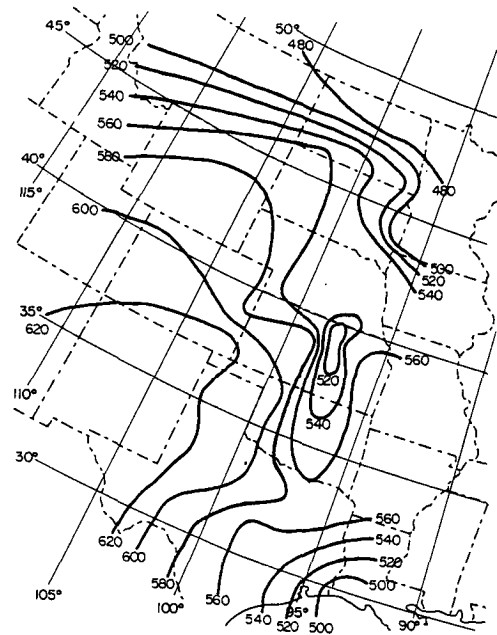


FIG. 3. The surface global solar radiation ( $W m^{-2}$ ) averaged for three summer months (June–August, 1977) as obtained by the GPAC observations during the 1977 summer experiment and supplemented by NOAA stations.

*c. The net radiation field at the top of the atmosphere*

In order to compute the net radiation budget at the top of the atmosphere, radiation energy data from NOAA 5 for the summer of 1977 were obtained from NOAA/EDIS. Each hemisphere is contained in a  $125 \times 125$  array. The data fit the intersections of a square mesh overlaid on a polar stereographic projection where array (63, 63) lies on the pole. We extracted a window over the Great Plains. A procedure developed at NOAA/NESS was used to allow transformation from geographical coordinates into grid points. It was found that our area of interest is covered by grid points 85–99 from north to south and 48–56 from west to east. A daily set of data contains four radiation fields, 1) daytime outgoing longwave radiation, 2) absorbed solar radiation, 3) available solar radiation and 4) nighttime outgoing longwave radiation.

The net radiation at the top of the atmosphere was computed using the average of the daytime and nighttime longwave outgoing radiation. The results are illustrated in Fig. 4. A parameter of variability defined as  $\sigma/F$ , where the standard deviation ( $\sigma$ ) is normalized by the mean field ( $F$ ) at each point, was computed and is presented in Fig. 5. To illustrate the difference between the daytime and nighttime fields of the outgoing longwave radiation, the corresponding three-month averages are presented in Fig. 6. To facilitate the interpretation of the various radiation fields, the average planetary albedo is also presented (Fig. 7).

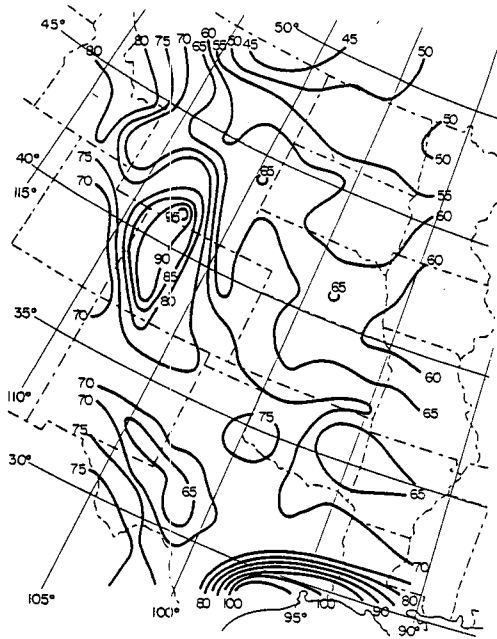


FIG. 4. Planetary net radiation ( $W m^{-2}$ ) averaged for three summer months (June–August, 1977) as obtained from the NOAA 5 scanning radiometer data stored on the (NMC)  $125 \times 125$  hemispheric grid.

3. Results and discussion

The net radiation fields at the surface (Fig. 2) and at the top of the atmosphere (Fig. 4) reveal remarkable similarity in their structure. It has been recognized that

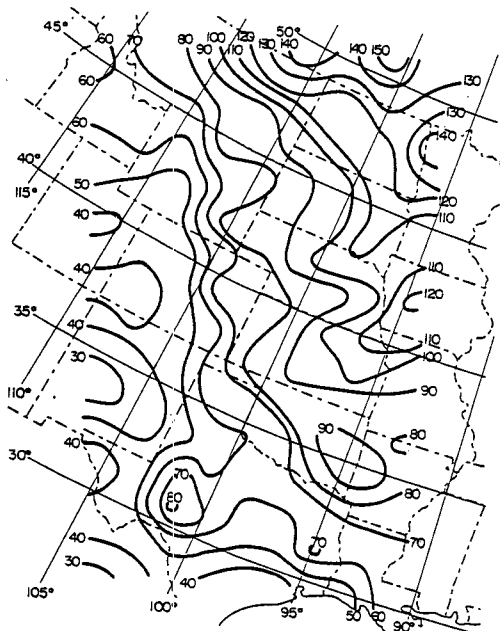


FIG. 5. Parameter of variability ( $\times 10^3$ ) for the planetary net radiation field as represented in Fig. 4.

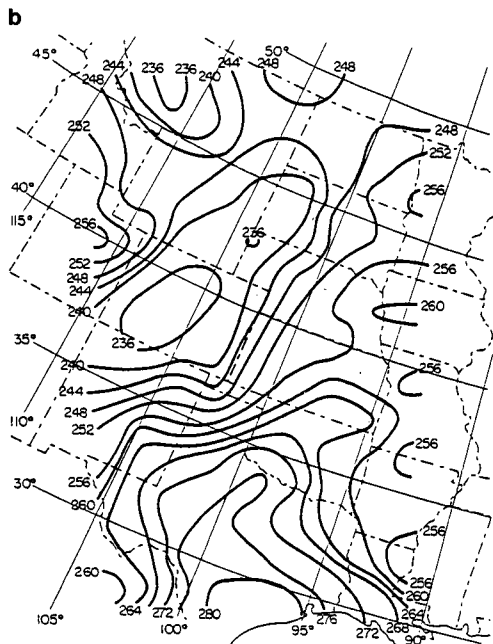
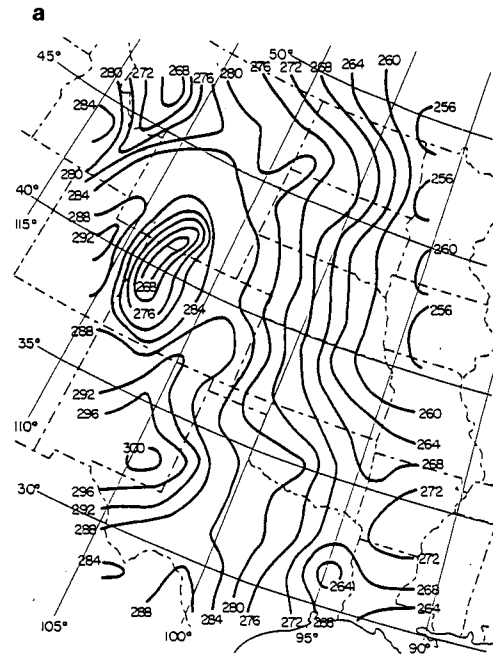


FIG. 6. Planetary (a) daytime and (b) nighttime outgoing longwave radiation ( $W m^{-2}$ ) averaged for three summer months (June–August, 1977) as obtained from the NOAA 5 scanning radiometer data stored on the (NMC)  $125 \times 125$  hemispheric grid.

clouds regulate these two fields. At the top of the atmosphere, the increased loss of energy to space by reflection from the clouds is offset by the decreased emission from the colder cloud tops. Therefore, in regions where the longwave outgoing flux is large, the

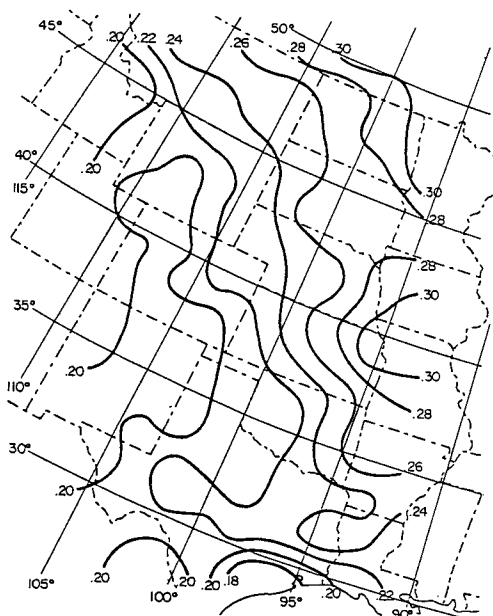


FIG. 7. The average planetary albedo (all conditions) averaged for three summer months (June–August, 1977) as obtained from the NOAA 5 scanning radiometer data stored on the (NMC)  $125 \times 125$  hemispheric grid.

net radiation will be low and vice versa (Figs. 4 and 6a). This interplay at the top of the atmosphere was discussed by various investigators (Schneider, 1972; Cess, 1976; Ohring and Clapp, 1980). They attempted to quantify the opposing albedo and greenhouse effects on the net radiation at the top of the atmosphere and for that purpose introduced the "Climate Sensitivity Parameter." There does not seem to be a consensus among the investigators as to which of the two effects is dominant; however, all agree that the two are compensating.

When the surface energy balance is considered, clouds act as modulators by decoupling the ground and space. Here, too, cloudiness affects the earth radiation balance in the longwave and shortwave wavelength in opposite ways; yet, the magnitude of these opposing effects is not well established. For instance, Linacre (1968) claims that clouds lower the net radiation intensity when it exceeds a critical value in the region of  $0.02 \text{ ly min}^{-1}$ , but increase it when the intensity is lower.

To better understand the structure of the two net radiation fields, the synoptic situation was investigated. For the months of July and August a very strong ridge located along the western Canadian coast and Alaska was responsible for cold air advection through west-central Canada and northern Plains states. This strengthened the thermal gradient near the northern border of the United States, and resulted in favorable conditions for storm development. Several stations in this area reported record or near record low August

mean temperature. Southward penetration of the cool air was limited by the relatively strong subtropical ridge over the Southeast (Dickson, 1977a,b). With the northwesterly polar jet position over west central Canada and north-central United States, the combined effects of a deep upper level trough over the north-central states, and a strong moisture-advecting high off the east coast, greater than normal precipitation totals were found in most areas east of the Continental Divide (see map of percentage of normal precipitation *Weekly Weather and Crop Bulletin*, 13 September 1977). This is also supported by the observed minimum of global solar radiation over Kansas (Fig. 3).

In the northern parts of the Great Plains, the isopleths of the global solar radiation are east–west oriented (Fig. 3); this would indicate a strong control of the migrating synoptic systems on the insolation. The orientation of the isopleths of the net solar radiation is similar, i.e., the global solar radiation dominates the net radiation balance.

At the top of the atmosphere, east of the  $110^\circ$  parallel, the east–west orientation of the net radiation isopleths is less pronounced than at the ground. West of the  $110^\circ$  parallel, the field of the planetary net radiation seems to be similar to the planetary daytime outgoing longwave radiation (Fig. 6a). These differences between the planetary and surface net radiation structure might be due to the different computational schemes. The planetary net radiation was computed from one observation per day in the visible while the global solar radiation is based on continuous observations. It is conceivable that in this region, the morning satellite observation is a poor indicator of the actual daily average. The corresponding parameter of variability of the planetary net radiation is relatively high, which might be due to the moving synoptic systems.

For the remaining parts of the Great Plains the surface net radiation and the global solar radiation fields are not similar in their structure. The minimum in global solar radiation over Kansas coincides with the area of over 150% of normal precipitation for the summer of 1977 (*Weekly Weather and Crop Bulletin*, 13 September 1977). The global solar radiation field around the  $105^\circ$  parallel shows high values in the predominantly clear and dry regions of Texas, New Mexico and Arizona. For the summer of 1977, this region had only 75% of normal precipitation and as such, was less cloudy than the average.

The net radiation fields at the top of the atmosphere and at the ground seem to be affected by, in addition to the solar forcing, also the topography. The low net radiation ( $185 \text{ W m}^{-2}$ ) in the clear desert regions is a result of the combined effects of large surface albedos ( $\sim 24\%$ ) and large radiative cooling under predominantly clear sky. In the mountain regions, we find a maximum net radiation ( $235 \text{ W m}^{-2}$ ) which is a result of the combined effects of small surface albedos ( $\sim 16\%$ ) and small radiative cooling. This smaller ra-

diative cooling is possibly due to the higher elevations (lower radiative temperatures), and trapping of the emitted radiation by the mountain ranges. The plausibility of the strong influence of the ground topography on the net radiation balance is supported by the spatial structure of the parameter of variability of the planetary net radiation (Fig. 5). Similar low values dominate these two regions implying that the balance is dictated by steady features rather than transient ones. The field of the planetary daytime outgoing radiation is coherent with the field of the net radiation. There is a well defined relative minimum over the mountain region and a well defined maximum over the clear desert region. However, the nighttime field of the emitted longwave radiation differs from the daytime field; in particular, the distinct maximum over the desert area is missing. It is well known, that areas that warm up faster will also cool faster. Evidently, during the nighttime satellite passage, the warmest parts of the desert cooled sufficiently to diminish the temperature gradients in respect to the surrounding areas. The higher elevations still maintain a relative minimum; however, the gradients are smaller and so are the gradients between the mountain and desert regions.

Various studies dealing with planetary radiation budgets from satellites (e.g., Stephens *et al.*, 1981) have demonstrated that the planetary albedo displays a maximum where there is a minimum in the emitted longwave flux. This did not seem to apply everywhere in the area of our study. Along the 105° parallel, south of 45°N (Fig. 7), the average of planetary albedo seemed to be the same (possibly due to different reasons). Yet, the outgoing longwave radiation was higher over the desert region than over the mountain region.

In order to quantify the similarity of the net radiation fields, the following regression analyses were performed:

$$\text{GNET} = a + b(\text{PNET}) \quad (5a)$$

$$\text{GNET} = a + b(\text{PNET}) + c(\text{PNET})^2 \quad (5b)$$

$$\text{GNET} = a + b(\text{PNET}) + c(\text{LWD}), \quad (5c)$$

where GNET is the net radiation at the ground, PNET, the net radiation at the top of the atmosphere (planetary) and LWD, is the daytime outgoing longwave.

The first two forms seemed to suggest themselves from the scattergrams initially plotted for the two fields. The third form was stipulated by Fig. 6a. Since the net radiation at the top of the atmosphere was computed on the NMC grid, the surface values were first interpolated to the same grid points. However, several grid points, in regions where observations were sparse, especially in mountain areas and along the coastline (where larger spatial variability can be expected) were eliminated from the analysis. Out of a total of 135 grid points, 59 were eliminated (Fig. 2). The results of the regression analyses are presented in Table 1. As evident from the table, the first-order

TABLE 1. Summary of regression analyses between ground net radiation (GNET) and planetary net radiation (PNET) and daytime longwave radiation (LWD) as expressed by Eqs. 5a-c.

	Multiple R	Simple R	R squared
PNET	—	0.688	0.474
Regression equation (5a) GNET = 101.814 + 1.195 (PNET)			
PNET	0.688	0.688	0.474
PNET <sup>2</sup>	0.688	0.688	0.474
Regression equation (5b) GNET = 0.484 + 0.374 (PNET) + 0.601 × 10 <sup>-4</sup> (PNET) <sup>2</sup>			
PNET	0.688	0.688	0.474
LWD	0.757	0.627	0.573
Regression equation (5c) GNET = 0.467 × 10 <sup>2</sup> + 0.285 (PNET) + 0.862 (LWD)			

regression and the second-order regression between the surface net radiation (GNET) and the planetary net radiation (PNET), yield the same correlation coefficient of 0.69. The multiple regression between the independent variable (GNET) and the dependent variables (PNET) and the daytime outgoing longwave radiation (LWD) yields a correlation coefficient of 0.76; the variables (PNET) and (LWD) are individually strongly correlated to the (GNET), the correlation coefficients being 0.69 and 0.63 respectively.

Several approximations were applied in the process of deriving the daily net radiation fields. For instance, the global solar radiation at the ground was computed from hourly observations, but the net longwave radiation was obtained from an empirical model based on average daily screen level temperature (computed from the daily minimum and maximum), and average daily cloud amount. The solar radiation observing stations and those that observe the necessary meteorological data were not always collocated. We accepted pairs that were up to 20 km apart. Also, the net radiation at the top of the atmosphere is derived from one observation per day in the visible and two observations per day in the IR. These approximations might have introduced errors that cannot be estimated easily.

#### 4. Summary

In this study, an attempt was made to obtain and compare the simultaneous fields of net radiation at the ground and at the top of the atmosphere. Satellite observations from NOAA 5 were utilized to relate planetary radiation budget parameters to surface net radiation over the central United States. The net radiation and the outgoing daytime longwave radiation at the top of the atmosphere were found to be correlated to the net radiation at the surface, yielding a multiple correlation coefficient of 0.76.

Our study demonstrated that the average planetary albedo is not always the best indicator of the emitted longwave flux. For instance, over New Mexico, Colorado and part of Wyoming the average planetary albedo seemed to be the same, yet the outgoing longwave radiation was higher over the desert region compared to that over the mountain region.

It was also evident that the surface global solar radiation is not the sole regulator of the net radiation. The net radiation is often derived from the global solar radiation via a regression formalism; as evident from our study, this might not be a good approximation in every climatic region.

With all the limitations cited, it would be difficult to ignore the striking structural similarity between the two fields of net radiation and further investigations on this subject seem to be appropriate.

*Acknowledgment.* We are indebted to Drs. A. Gruber and J. D. Tarpley for the numerous helpful discussions and to James M. Strayer for his skillful programming assistance in consolidating the diversified data sources. This research was supported by the NOAA/NESS AGRISTARS project under Grant NA80AA-D-0048 to the University of Maryland. The Computer Science Center of the University of Maryland provided additional computer time.

#### REFERENCES

- Abel, P. G., and A. Gruber, 1979: An improved model for the calculation of longwave fluxes at 11  $\mu\text{m}$ . NOAA Tech. Memo. NESS 106, 24 pp.
- Brunt, D., 1932: Notes on radiation in the atmosphere. *Quart. J. Roy. Meteor. Soc.*, **58**, 389-420.
- Budyko, M. I., 1974: *Climate and Life*. Academic Press, 508 pp.
- Cess, R. D., 1976: Climate change: An appraisal of atmospheric feedback mechanisms employing zonal climatology. *J. Atmos. Sci.*, **33**, 1831-1843.
- Dickson, R. R., 1977a: Weather and circulation of July 1977. *Mon. Wea. Rev.*, **105**, 1343-1348.
- , 1977b: Weather and circulation of August 1977. *Mon. Wea. Rev.*, **105**, 1481-1486.
- Gandin, D. R., 1970: The planning of meteorological station networks. WMO Rep. No. 265. TP. 149, 35 pp.
- Gruber, A., 1978: Determination of the earth-atmosphere radiation budget from NOAA satellite data. NOAA Tech. Rep. NESS 76, 28 pp.
- Hare, F. K., 1980: Long-term annual surface heat and water balances over Canada and the United States south of 60°N: Reconciliation of precipitation, run-off and temperature fields. *Atmos.-Ocean*, **18**, 127-153.
- Idso, S. B., and R. D. Jackson, 1969: Thermal radiation from the atmosphere. *J. Geophys. Res.*, **74**, 5397-5403.
- Kung, E. C., R. A. Bryson and D. H. Lenschow, 1964: Study of a continental surface albedo on the basis of flight measurements and structure of the earth's surface cover over North America. *Mon. Wea. Rev.*, **92**, 543-564.
- Lettau, H., 1969: Evapotranspiration climatology. I. A new approach to numerical prediction of monthly evapotranspiration, run-off, and soil moisture storage. *Mon. Wea. Rev.*, **97**, 691-699.
- Linacre, E. T., 1968: Estimating the net-radiation flux. *Agric. Meteor.*, **5**, 49-63.
- Monteith, J. L., 1961: An empirical method for estimating longwave radiation exchanges in the British Isles. *Quart. J. Roy. Meteor. Soc.*, **87**, 171-179.
- NASA, 1979: *Earth Radiation Budget Science 1978*. Proc. of a workshop held at Williamsburg, VA, NASA Conf. Pub. 2100, 72 pp.
- Ohring, G., and P. Clapp, 1980: The effect of changes in cloud amount on the net radiation at the top of the atmosphere. *J. Atmos. Sci.*, **37**, 447-454.
- Schneider, S. H., 1972: Cloudiness as a global climatic feedback mechanism: The effects on the radiation balance and surface temperature of variations in cloudiness. *J. Atmos. Sci.*, **29**, 1413-1422.
- Sellers, W. D., 1965: *Physical Climatology*. University of Chicago Press, pp. 53-81.
- Stephens, G. L., G. G. Campbell and T. H. Vonder Haar, 1981: Earth radiation budgets. *J. Geophys. Res.*, **86**, 9739-9760.
- Tarpley, J. D., 1979: Estimating incident solar radiation at the surface from geostationary satellite data. *J. Appl. Meteor.*, **18**, 1172-1181.
- , S. R. Schneider, J. E. Bragg and M. P. Waters, III, 1978: Satellite data set for solar incoming radiation studies. NOAA Tech. Memo. NESS 96, 36 pp.
- Willmott, C. J., E. Vowinckel and S. Orvig, 1978: A modified digital model for predicting energy budgets in the United States. *Pub. Climat.*, **31**, 62-63.
- Winston, J. S., A. Gruber, T. I. Gray, Jr., M. S. Varnadore, C. L. Earnest and L. P. Mannello, 1979: Earth's atmosphere radiation budget analyses derived from NOAA satellite data June 1974-February 1978. Vols. 1 and 2, U.S. Dept. of Commerce, NOAA/NESS, Washington, DC.